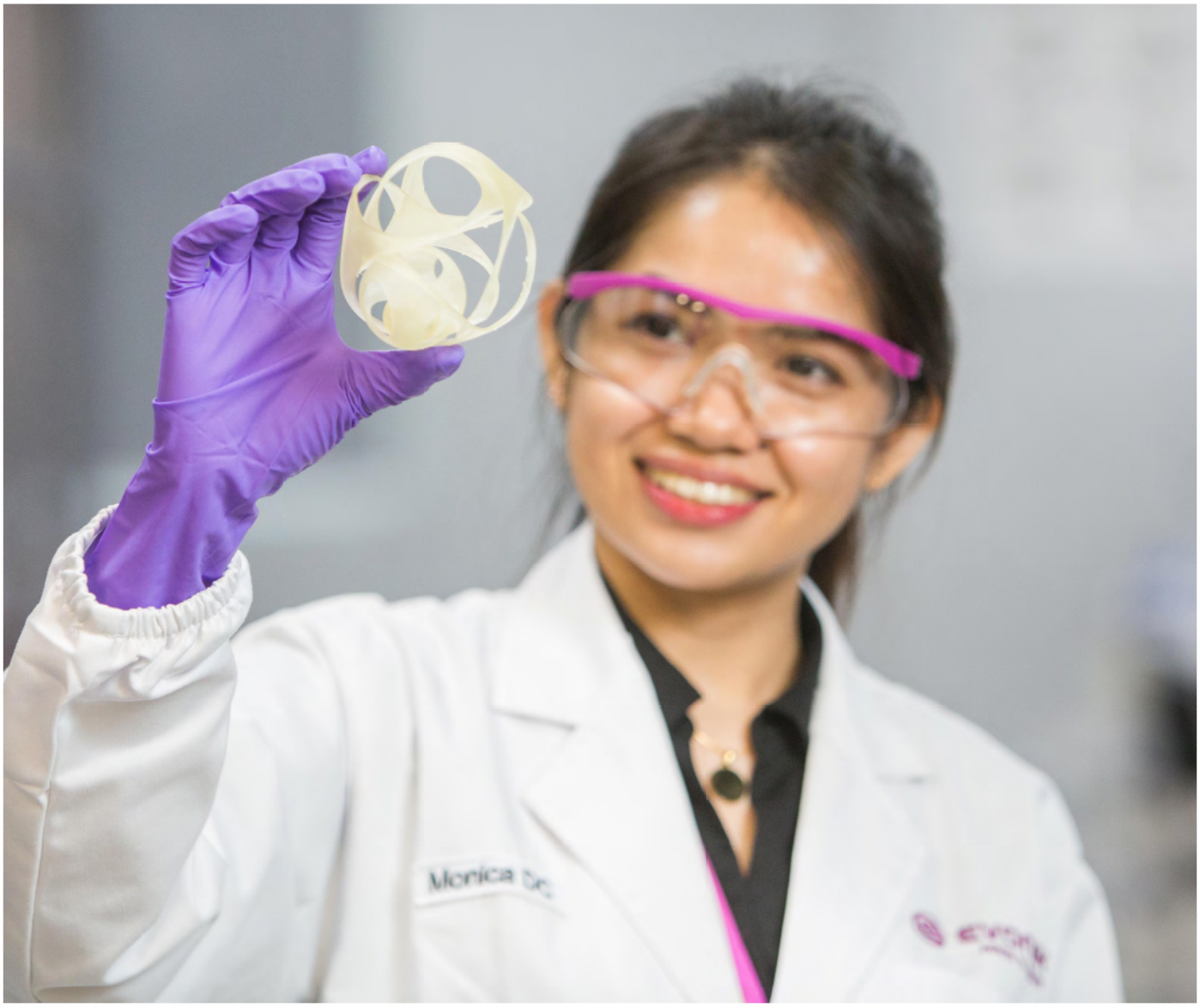

Pushing the boundaries of chemistry? It takes #HumanChemistry

Make your curiosity and talent as a chemist matter to the world with a specialty chemicals leader. Together, we combine cutting-edge science with engineering expertise to create solutions that answer real-world problems. Find out how our approach to technology creates more opportunities for growth, and see what chemistry can do for you at:

evonik.com/career

EVONIK
Leading Beyond Chemistry

Received: 3 September 2021 | Revised: 24 November 2021 | Accepted: 22 December 2021

DOI: 10.1002/app.52141

ARTICLE

Applied Polymer SCIENCE WILEY

Devulcanization of ethylene-propylene-diene monomer rubber waste. Effect of diphenyl disulfide derivate as devulcanizing agent on vulcanization, and devulcanization process

Larissa Gschwind[1] | **Carmen-Simona Jordan**[1] | **Norbert Vennemann**[2]

[1]Faculty of Management, Culture and Technology, University of Applied Sciences Osnabrueck, Lingen, Germany

[2]Faculty of Engineering and Computer Science, University of Applied Sciences Osnabrueck, Osnabrueck, Germany

Correspondence
Carmen-Simona Jordan, Faculty of Management, Culture and Technology, University of Applied Sciences Osnabrueck, D-49809, Lingen, Germany.
Email: s.jordan@hs-osnabrueck.de

Funding information
German Federal Environmental Foundation, Grant/Award Number: 34250/01-21/0

Abstract

A systematic study was performed to understand the effects of the devulcanizing agent dibenzamido diphenyl disulfide (DBD) on the vulcanization and devulcanization process of a sulfur-cured ethylene-propylene-diene monomer (EPDM) rubber. The influence of DBD on vulcanization was investigated by mixing DBD with virgin rubber and curative system. The devulcanization of rubber waste was achieved with varying amounts of DBD ranging from 0.4 to 13.8 wt% and temperatures from 150 to 200°C. The quality of vulcanizates and devulcanizates was evaluated by rheometer tests, temperature scanning stress relaxation measurements, and analysis of mechanical properties. During vulcanization, DBD acts as an accelerator in the presence of sulfur. When accelerators are added, the scorch time increases, and the cure rate decreases. Thus, DBD acts as a retarder. In the presence of activators, DBD leads to a significant reduction of crosslink density. This results in composites with high elongation at break and poor compression set values. The efficiency of the devulcanization of rubber waste depends strongly on DBD concentration and temperature. The monosulfidic crosslinks are cleaved by low concentrations of DBD, while polysulfidic crosslinks require higher concentrations. These results show that DBD is effective as a devulcanizing agent and degrades the network below 200°C.

KEYWORDS

EPDM rubber waste, devulcanization, disulfide, TSSR, vulcanization

1 | INTRODUCTION

The recycling of rubber waste is still considered a challenge due to its chemically cross-linked three-dimensional structure. Intensive studies have been carried out in the last decades to break down the crosslinked rubber network by devulcanization. This involves treating rubber waste thermo-mechanical,[1,2] chemically,[3–5] biologically,[6–8] with ultrasound[9,10] and microwaves,[11,12] or by a combination[13] of such methods to achieve selective cleavage of C-S and S-S bonds without additional damage of C-C bonds in the polymer backbone. Devulcanization as a reversible

process of vulcanization is the standard processing method for the material recovery of rubber waste. In the ideal case, a melt-processable material is obtained after devulcanization, which can later be used to produce new industrial rubber goods and composites.[14,15] Despite all efforts in current rubber waste recycling research, the selectivity of S-S cleavage is challenging to achieve. Therefore, poor quality of the recycled material is often the result.[16] The efficiency of devulcanization is influenced by the type and amount of sulfidic crosslinks in the elastomer.[17,18,19] To better understand the mechanism of the devulcanization process and the function of devulcanizing agents (DAs), several models have been proposed. The main difficulty in elucidating the mechanism at the molecular level is the complexity of the devulcanization process due to various phenomena co-occurring and the large number of chemicals used in a rubber compound.[20] Besides, side reactions and crosslinks can occur depending on the DA and the devulcanization parameters.[17,18,21]

One of the first mechanisms for thermo-mechanical devulcanization under shear was formulated by Mouri et al.[22] In the case of sulfur-crosslinked rubbers, the heat converts the polysulfidic (PS) and disulfidic (DS) crosslinks into monosulfidic (MS) crosslinks.[22,23] The shear is used to cleave the MS crosslinks. Another model for selective network scission by thermo-mechanical devulcanization is based on different elastic constants and binding energies of S-S, C-S, and C-C bonds.[24,25] The differences between the binding energies are minor, and a purely thermal process leads to unselective cleavage. Since the elastic constant of S-S bonds is much smaller than that of C-C bonds, S-S bonds are the most extended under shear. As a result, the elastic energy generated by shear stress is most significant at S-S bonds leading to selective cleavage of crosslinks. However, this cleavage occurs only at high shear stress; otherwise, the entropic effect predominates.

By treating rubber waste particles with heat and pressure, as in the case of high-pressure high-temperature sintering (HPHTS), the devulcanization occurs by rearrangement of crosslinking bonds.[26] During the sintering process, heat is required to provide energy to break the bonds, and pressure brings the particles into close contact. The rearrangement on the particle surface and within the particles leads to new crosslinking sites, which results in one single piece of rubber. Using dienophiles or dipolar organic additives during HPHTS improves the recycled natural rubber (NR), as reversion is slowed down, the main factor for property losses.[27]

Physical devulcanization methods, such as thermo-mechanical, ultrasonic or microwave techniques, are often combined with chemicals to increase selective network scission.[28–31]

Depending on the type of DA, the degradation of the network is either nucleophilic, radical, or in the case of inorganic systems like phenylhydrazine chloride oxidative.[3,32] In the presence of a free accelerator, the mechanism is a substitution reaction, where the rubber molecule on one side of the crosslinking site is exchanged with part of the accelerator.[32] These reactions could be compared to metathesis reactions used in materials with self-assembling properties.[33]

The devulcanization with amines is according to a nucleophilic mechanism.[34] However, high temperatures and the excess of amines break the cyclic form of sulfur (octa form) and promote re-crosslinking.[17] Furthermore, amine like hexadecylamine (HDA) degrade less PS bonds because it forms complexes with zinc ions that stabilize the PS bonds. HDA is an effective DA at temperatures between 200 and 350°C.[35]

The radical degradation of PS crosslinks occurs easier than that of MS crosslinks due to different binding energies.[36,37] Movahed et al. suggested that 2-mercaptobenzothiazole disulfide and the polymer chain are cleaved under shear force.[38] The disulfide radical then reacts with the polymer radical. The devulcanization with diallyl disulphide,[39] tetrabenzyl thiuram disulphide,[40] bis (3-triethoxysilyl propyl) tetra- sulphide,[41] or the DeLink[42] proceeds according to a similar mechanism. In contrast, Joseph et al. proposed a radical mechanism, with diphenyl disulfide (DPDS) acting as a cleavage reagent rather than a free radical scavenger for the scission of an NR network.[32] Devulcanization of EPDM with disulfides was performed at temperatures higher than 200°C.[18,31,43,44] Compared to 100% rubber waste powder, the mechanical properties were improved and were not significantly decreased when compounded with more than 50% virgin rubber. In the case of virgin rubber blended with DPDS devulcanized NR, the properties were even better than the properties of the raw rubber.[45]

The mentioned issues show that the devulcanization parameters and the type and concentration of DAs can lead to either degradation or crosslinking of the rubber waste network. In general, the path of rubber proceeds from vulcanization to devulcanization back to re-vulcanization. The term re-vulcanization describes the process of vulcanization after devulcanization. Devulcanization approach to improve is necessary to understand the function of DAs during devulcanization and re-vulcanization. The devulcanization mechanisms are complex, and simplified models are needed to represent and understand the processes.

Based on the previous remarks, two model systems are studied in this work to provide more information on the effects of DBD on network formation (vulcanization) and network degradation (devulcanization). The

influence of DBD on the network formation during vulcanization was investigated on samples consisting of virgin EPDM rubber, carbon black, oil, curative system, and different 2 wt% of DBD. The DBD interaction with each component of the curing system was studied and compared with the formulation without DBD. This model system helps to understand how residues of DBD behave during re-vulcanization and how DBD interacts with the residues of the curative system in the rubber waste during devulcanization. The effect of DAs on network degradation was analyzed by mixing rubber waste particles (RWP) with different amounts of DBD. For this purpose, thermo-chemical devulcanization was carried out in a heating press to eliminate external factors such as shear and atmospheric air, which further affect the devulcanization and complicate the mechanism. Curing characteristics and mechanical properties of resulting composites were evaluated. Furthermore, temperature scanning stress relaxation (TSSR) measurements were performed to examine the network structure and crosslink density. The gained knowledge can be used for recycling rubber waste to produce a high-quality, usable secondary raw material.

2 | EXPERIMENTAL

2.1 | Materials

Sulfur vulcanized EPDM rubber waste with a particle size distribution between 250 and 850 μm and a density of 1.1 g/cm^3 were obtained by milling at room temperature from M.D.S. Meyer GmbH, Germany. The main components of the rubber waste are EPDM raw rubber Keltan 9650Q (Lanxess GmbH, Germany), Carbon Black of type N550 (Avokal GmbH, Germany), and paraffinic oil Mabanol Base oil 500 MSN (Mebanol GmbH & Co. KG, Germany). The curing system consists of sulfur (S) from Melos GmbH Germany, Stearic acid (SAc) supplied by Carl Roth GmbH & Co. KG Germany, Zinc oxide (ZnO) from Melos GmbH Germany, Zinc bis(dibenzyl dithiocarbamate) (ZBEC) from Weber & Schaer GmbH & Co. KG, and N-cyclohexyl-2-benzothiazole-sulfenamide (CBS) from Sun & Bright Industrial Ltd., China. The devulcanized agent Dibenzamido diphenyl disulfide (DBD) was provided by Schill & Seilacher GmbH, Germany.

2.2 | Methods

Thermogravimetric Analysis was carried out using a TG 209 F1 Libra® from Netzsch-Gerätebau GmbH, Germany. The heating rate was 2 K/min, and argon was used from room temperature to 650°C, while oxygen was used from 650 to 900°C. The temperature was held for 5 min each for argon and oxygen at 650°C.

2.2.1 | Sample preparation and compounding

The formulation of samples S1–S5 is given in Table 1 and should mimic that of RWP. Sample 5 has the same composition as RWP. The samples are obtained in a

TABLE 2 Formulations of the rubber compound S6–S11

	Amount in wt%					
	S6	**S7**	**S8**	**S9**	**S10**	**S11**
RWP	100	99.6	98.0	96.1	92.6	86.2
DBD	0	0.4	2.0	3.9	7.4	13.8

TABLE 1 Formulations of the rubber compound S1–S5

Sample no. designation	S1, BC/ZS	S2, BC/S	S3, BC/ZS/S	S4, BC/Acc	S5 (reference), BC/ZS/Acc/S
Ingredients	Amount in phr (per hundred rubber)				
EPDM	100	100	100	100	100
Carbon black	120	120	120	120	120
Oil	100	100	100	100	100
ZnO	4	—	—	4	4
SAc	2	—	—	2	2
CBS	—	—	2.5	—	2.5
ZBEC	—	—	0.7	—	0.7
Sulfur	—	1.2	1.2	1.2	1.2

Abbreviations: Acc, accelerator (CBS and ZBEC); BC, base compound (EPDM, carbon black, oil); S, sulfur; ZS, ZnO plus SAc.

laboratory internal mixer type Haake PolyLab QC from ThermoScientific, Germany. 90°C, 40 rpm, and a fill factor of 0.7. After 15 min of mixing raw EPDM, carbon black, and oil, a curative system was added. The curative system is systematically varied.

The samples S7–S11 were prepared using RWP and different amounts of DBD, according to Table 2 in a household mixer KCC9061S at room temperature for 10 min. Sample 6 consists of only RWP.

2.2.2 | Cure behavior

The curing characteristics were analyzed by DIN 53529–1/−2/−3:1983 using a Dynamic Moving Die Rheometer Type D-MDR 3000 from MonTech Werkstoffprüfmaschinen GmbH, Germany. The samples S6-S11 are in powder form, making it impossible to die-cut the samples with a defined volume. The samples were prepared according to the standard for the rheometer test method: 4 g of rubber waste powder was formed to pile and put between two plastic foils and vulcanized for 30 min at 180°C. In addition to studying temperature's influence on the network degradation, sample 9 was tested at 150, 160, 170, 180, 190, and 200°C.

2.2.3 | Preparation of test plates for thermo-chemical experiment

The samples S1a–S5a with a constant amount of 2 wt% DBD were prepared analogously to S1–S5 as plates of 2 mm thickness by compression molding at 180°C and 10 MPa with an electrical heated hydraulic press Polystat 200 T from Schwabenthan, Germany.

According to standard procedure, samples S3 and S5a were cured with the t_{90} cure time + 2 min, obtained from D-MDR measurements for 30 min vulcanized time. The usual curing time t_{90} could not be determined for samples S2, S2a, S3a, S4, S4a, and S5, respectively. The vulcanization is still not achieved after 120 min (see supporting materials A1). The vulcanization is very slow when the curative system is not complete. The results of samples S2–S5 without DBD and S2a–S5a with DBD are shown in Table 3. Samples S6–S11 consisting of RWP were treated for 15 min in the heating press using the conditions described below. For this sample, the vulcanization and devulcanization take place at the same time.

2.2.4 | Characterization of EPDM rubber waste particles

The particle size distribution (PSD) shown in Figure 1 is similar to PSD reported by Hoyer et al.[46] when rubber waste is ground by ambient temperature.

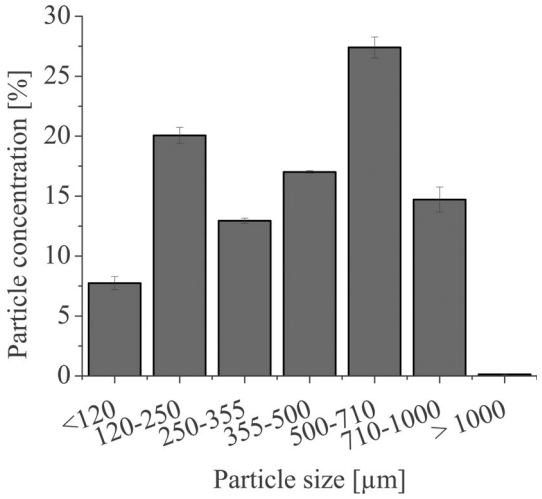

FIGURE 1 Particle size distribution of rubber waste particles used for devulcanization

Samples	t_{90} (min)	M_H (nm)	M_L (nm)	ΔM (nm)	t_{S2} (min)
S2 (BC/S)	(26.1[a])	4.1	1.8	2.2	26.1
S2a (BC/S/DBD)	(27.4[a])	4.8	1.7	3.1	21.4
S3 (BC/Acc/S)	2.0	8.2	1.6	6.6	1.2
S3a (BC/Acc/S/DBD)	(22.5[a])	6.5	1.6	4.9	2.8
S4 (BC/ZS/S)	(14.9[a])	12.2	1.7	10.4	1.8
S4a (BC/ZS/S/DBD)	(22.1[a])	7.8	1.6	6.2	6.2
S5 (BC/ZS/Acc/S)	(10.0[a])	14.8	1.5	13.3	1.2
S5a (BC/ZS/Acc/S/DBD)	4.4	8.7	1.4	7.3	1.6

TABLE 3 Results of rheometer tests obtained from samples S1–S5 (without DBD) and S1a–S5a (with 2.0 wt% DBD)

[a]The values in brackets indicate t_{90}-values which were not determined according to DIN 53529. Due to very slow cure and marching modulus, a plateau or maximum value of the cure curve was not approached by far, even after 2 h of testing. Therefore, the torque obtained after 30 min was used as maximum torque to calculate the corresponding t_{90}-values, alternatively.

The thermogravimetric analysis (TGA) Figure 2 shows the decomposition temperature of three main components of RWP: EPDM, oil, and carbon black.

The mass loss of around 300°C belongs to the paraffinic oil, at 460°C to EPDM and 650°C to carbon black (Figure 2a). The same results were reported by Lepadatu et al.[47] and Pistor et al.[11] The mass loss of S5 and RWP, is shown in Figure 2b. A slight difference in the mass loss is observed despite the exact composition of the samples S5 and S6. This can be due to the partial degradation of oil in the rubber waste powder.

2.2.5 | Characterization of network structure and crosslinking density

TSSR measurements were performed according to ASTM D8363-20 using a TSSR instrument from Brabender GmbH, Germany. Tests were performed in the temperature range from 23 to 240°C at a 2 K/min heating rate and a constant strain of 30%. The dumbbell-shaped test specimens were conditioned for 2 h at 23°C.

According to ASTM D8363-20, crosslink density can be deduced from TSSR-measurements by considering the initial slope of the stress-temperature curve. This method is based on the neo-Hookean material model, which applies well to ideal rubber. Furthermore, instead of the initial slope of the stress-temperature curve, the absolute value of initial stress was used to calculate Equation (1).

$$\nu = \frac{\sigma}{R * T * \left(\lambda - \lambda^{-2}\right)} \quad (1)$$

The trace of the temperature-dependent relaxation spectrum also obtained from TSSR measurements gives information about the network structure of the samples. PS bridges are chemically degraded at lower temperatures, and MS and DS bridges are degraded at higher temperatures, as the thermal stability decreases with the length of the sulfur bridges.[48]

2.2.6 | Characterization of mechanical properties

Tensile tests were carried out according to DIN 53504:2009 with a universal testing machine Zwick 1120 from Zwick GmbH & Co. KG, Germany, on three dumbbell-shaped test specimens. The preload was 1 N, and the constant speed was 200 mm/min. The compression set was measured according to DIN ISO 815-1/-2:2016 at 70°C and for 24 h on one test piece. Therefore, three specimens (13 mm diameter and 2 mm thick) were stacked on top of each other.

3 | RESULTS AND DISCUSSION

3.1 | Influence of DBD on network formation

DBD was combined with different component groups of a curative system–activator, accelerator, and sulfur–and the base compound EPDM, oil, and carbon black to understand the function of DBD during vulcanization. The cure time (t_{90}) after 30 min vulcanization, the maximum torque (M_H), the minimum torque (M_L), the difference $M_H - M_L$ (ΔM), and the scorch time (t_{S2}) are given in Table 3. The minimum torque is related to the viscosity of the samples, which is not affected by DBD.

The influence of DBD in combination with the curative system on cure behavior at 180°C vulcanization temperature is depicted in Figure 3.

Without sulfur (S1), the rheometer torque does not increase (Figure 3a), that is, vulcanization does not occur, as expected. The addition of DBD (S1a) also shows no crosslinking reaction, although disulfides can act as sulfur donors and, in combination with activators and fatty acids, lead to crosslinking.[49] In the presence of sulfur without activators (S2) a slight increase of torque is recognizable. The reaction rate is very slow, which is typical for non-accelerated sulfur vulcanization.

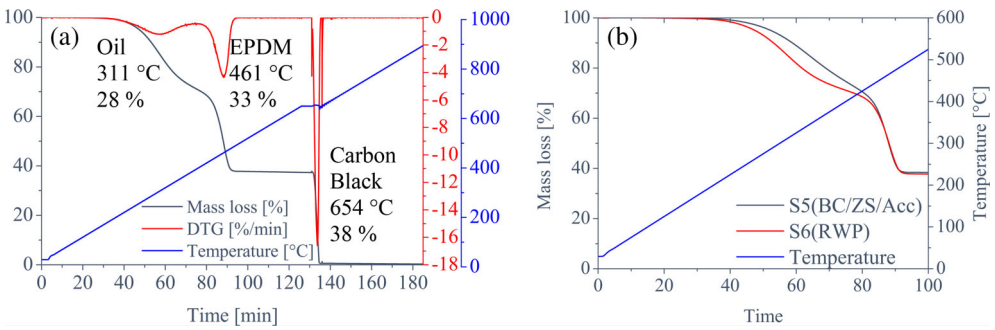

FIGURE 2 Mass loss and DTG curve of rubber waste particles [Color figure can be viewed at wileyonlinelibrary.com]

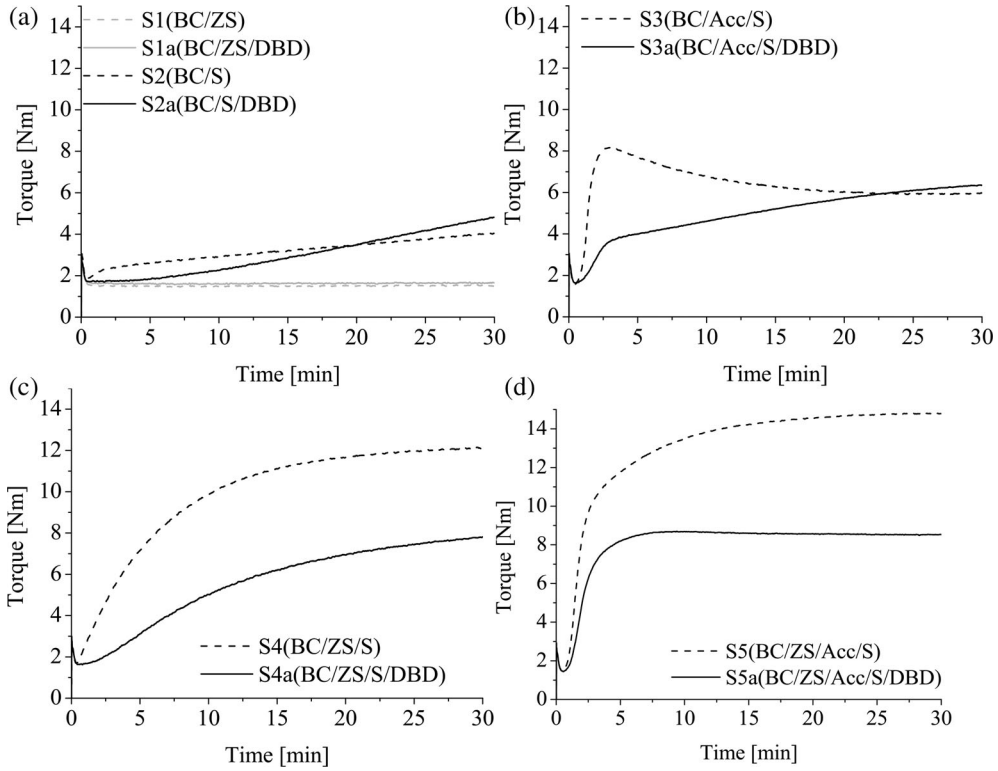

FIGURE 3 Influence of DBD in combination with the curative system on cure behavior at 180°C

When DBD was added (S2a), the scorch time t_{S2} and the curve slope increased slightly, indicating an accelerating effect of DBD. Vega et al. reported that DPDS has an accelerating effect in the presence of sulfur and leads to devulcanization of squalene above 200°C.[50] When accelerators and sulfur (S3) were combined, the slope of the rheometer curve was steep, which is related to a fast vulcanization reaction (Figure 3b). After reaching the maximum torque, a decrease of torque indicates reversion of the crosslinking reaction, as it is typical for networks consisting of PS crosslinks.[36] Addition of DBD (Sa3) reduces the reaction rate and increases the scorch time t_{S2}. DBD radicals may interact with CBS/ZBEC during the formation of the active sulfurating agent or by reacting with the crosslink precursor,[36] preventing the crosslinking reaction and resulting in a longer scorch time. It appears that DBD has more of an inhibitory effect when other accelerators are present. Furthermore, reversion of the cure reaction is prevented by the addition of DBD, and instead, a slight increase of the torque, also known as marching modulus, appears in the trace of the rheometer curve.

The rheometer curve of S4 in Figure 3c shows a moderate reaction rate and no reversion. The scorch time is low, that is, the vulcanization reaction starts immediately. Both M_H and ΔM are almost at the level of sample S5, which contains the entire curative system. Since activators incorporate shorter sulfur chains and thus more sulfur is available for further crosslinking,[36] the high ΔM is expected, as ΔM is related to the crosslink density. In addition, shorter sulfur bridges MS and DS do not tend to revert.[36] When DBD was added (S4a), the maximum torque M_H and consequently ΔM decreases by almost half, which means the crosslink density decreases. Furthermore, DBD leads to an increase in scorch time t_{S2} and a decrease in the reaction rate. DBD acts again as an accelerator and forms an active sulfurating agent with sulfur and the activators, resulting in a high scorch time. Although DBD has an accelerating effect, its effectiveness is relatively low compared to CBS/ZBEC, which explains the low reaction rate. However, vulcanization reaction with DBD and sulfur in the presence of activators is improved compared to the vulcanization reaction without activators (S2a).

In Figure 3d, the rheometer curve of sample S5 is presented. The composition of S5 is the same as for RWP; typical sulfur cured elastomer with an efficient vulcanization system (EV). It could be considered as a reference. The combination of accelerator and activators leads to a sharp increase in the curve and a high ΔM implying a fast vulcanization reaction and a high crosslink density. A typical EV system consists of a sulfur/accelerator ratio of less than 0.5 and usually forms MS and DS bridges, and therefore no reversion takes place. DBD (S5a) increases the scorch time slightly and reduces ΔM, that is, the crosslink density. Since activators are responsible

for high crosslink densities,[17,51] the decrease in M_H and ΔM can be attributed to the interaction of DBD with activators. Furthermore, the vulcanization reaction is not affected because the slope in the initial part of the curve does not change. If other, more effective accelerators like CBS/ZBEC are present, these determine the vulcanization reaction.

3.1.1 | Effect on network structure and crosslink density

TSSR-measurements were performed on the S2–S5 and S2a–S5a samples to investigate the crosslink density and the network structure. The rheometer curves showed that samples S1 and S1a could not be vulcanized; no TSSR measurements were performed for these samples. The values of initial stress σ_0, T_{50}, and crosslink density υ are given in Table 4. The obtained values reflect the crosslink density of the rubber network and can be used for comparative purposes.

The influence of DBD interactions with the curative system by stress temperature and relaxation measurements (TSSR) are shown in Figure 4.

The normalized stress temperature curve of sample S5 is depicted in Figure 4d on the left. S5 exhibits a typical behavior of a fully cured rubber sample. The stress increases slightly with increasing temperature between 23 and 50°C due to the entropy effect. Around 50°C, the stress decreases somewhat, followed by a section up to 150°C where the stress increases linearly with temperature before a strong stress decay occurs at temperatures above 150°C. The intermediate decrease of stress in the temperature range of about 50°C reflects physical induced stress relaxation caused by polymer-filler interactions.[52,53] After desorption of the bound rubber layer around the filler particles, the entropy elastic properties of the sample lead again to an increase of stress before the stress drops down to almost zero caused by chemical-induced relaxation processes at high temperature.

In the relaxation spectrum of S5 (Figure 4d, right), the center of the S5 peak is located at about 200°C. This peak can be attributed to the cleavage of short sulfur bridges (MS and DS) resulting from the EV system. MS and DS bridges are thermally more stable, whereas PS bridges chemically degrade at lower temperatures.[48] Apart from crosslink density, the T_{50} value is another characteristic quantity of TSSR measurements (Table 4), equal to the temperature where the stress has decreased 50%. T_{50} gives information about the thermal stability of the network structure. S5 exhibits the highest T_{50} value, that is, the thermal stability of all samples (see Table 4). Sample S2 (Figure 4a) was cured only with sulfur but without any accelerator.

In contrast to S5 the sample S2 exhibits strongly stress relaxation, as is seen in the stress curve of Figure 2a. The stress decay starts directly at room temperature and overcompensates the entropy effect, and thus no stress increase is recognizable. The low crosslink density of S2 (Table 4) compared to S5 is the high-stress relaxation. The network structure is incomplete, and molecular motions of long-chain segments can occur under external stress. In the presence of DBD (S2a), a higher crosslink density is achieved, indicated by higher initial stress and reduced stress relaxation. As is typical for accelerators, more active crosslinking sites are formed than in sulfur vulcanization without accelerators, where sulfur is consumed by the formation of circular bonds or side chains.[36,54] In the relaxation spectrum of S2 and S2a a single peak appears at about 145°C. The relatively low peak temperature is typical for cleavage of PS and indicates that PS crosslinks predominate in both cases.

The addition of accelerators to sulfur (S3) leads to a more defined peak in the relaxation spectrum compared to S2 (Figure 4b), indicating a uniform network caused

TABLE 4 Results of TSSR tests obtained from samples S2–S5 (without DBD) and S2a–S5a (with 2.0 wt% DBD)

Samples	σ_0 (MPa)	T_{50} (°C)	υ^a (mol/m^3)
S2 (BC/S)	0.19	130.1	109
S2a (BC/S/DBD)	0.26	142.9	149
S3 (BC/Acc/S)	0.30	136.5	172
S3a (BC/Acc/S/DBD)	0.26	135.9	149
S4 (BC/ZS/S)	0.47	183.6	270
S4a (BC/ZS/S/DBD)	0.28	148.3	161
S5 (BC/ZS/Acc/S)	0.58	211.1	333
S5a (BC/ZS/Acc/S/DBD)	0.37	157.0	212

[a]Calculated according to Equation (1).

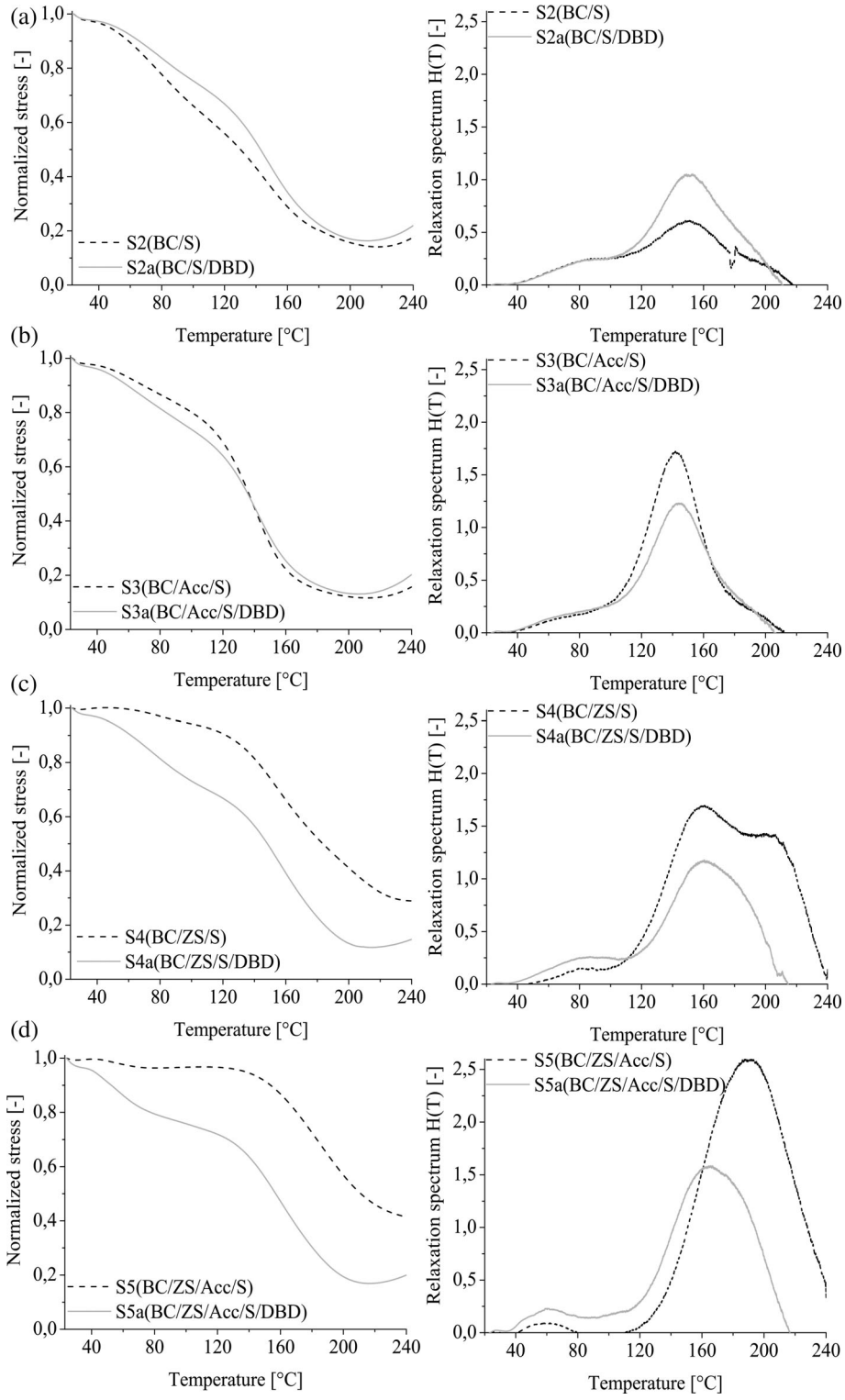

FIGURE 4 Influence of DBD in combination with curative system on TSSR stress temperature curves (left) and relaxation spectra (right)

by accelerators. Yet, the peak position has not changed, implying that the formed crosslinks are still PS. The stress relaxation is still high, which is due to the low crosslink density. DBD shows no effect on the network structure when the stress curve and relaxation spectrum of S3a are considered. The slight decrease in crosslink density (Table 4) can result from the t_{90} time, 4 min without DBD, and 24.5 min with DBD due to the marching modulus.

When activators and sulfur were combined (S4), the crosslink density strongly increased compared to S3 (Table 4). The stress curve shows less stress relaxation, indicating an almost fully formed network (Figure 4c). The double peaks in the relaxation spectrum at 150 and 200°C

suggest the formation of PS, MS, and DS crosslinks, respectively. Only in the presence of activators, the crosslink precursors consisting of an accelerator, sulfur, and polymer form after reaction with another polymer molecule again crosslink precursors, leading to further crosslinking sites with less sulfur atoms.[36] In contrast, DBD results in a reduction of crosslink density (Table 4). This manifests itself in the stress relaxation in the stress curve. In addition, T_{50} value and the shift of the relaxation peak to the left indicate a decrease in thermal stability of the crosslinks. DBD thus leads to predominantly PS bridges.

S5a shows the same characteristics as S4a. By adding DBD the stress relaxation and crosslink density decreases compared to S5 (Figure 4d and Table 4), and S5a shows no entropy elastic behavior. These points indicate that the network is not fully developed, and the plastic part is increased in contrast to the elastic part.[55] In the relaxation spectrum, the relaxation peak (Figure 4d) shifts to the left, and the T_{50} value (Table 4) decreases. Both are indications that the crosslinked species formed are thermally less stable PS crosslinks.

In summary, DBD leads to lower crosslink density and PS crosslinks even though activators are present when an EV system is used.

3.1.2 | Effect on mechanical properties

The mechanical properties are shown in Table 5 and compared with DIN EN 681–1: 2006 for O-ring sealing systems. The S5 and RWP samples were obtained according to the formulation of O-ring sealing system. As expected, the sample S5 achieves the values according to DIN EN 681–1: 2006. S5 has a tensile strength of 10.7 MPa and an elongation at break of 330%, which suggests a uniform and properly formed network in the vulcanized sample. The value of 9.9% of the compression set indicates high elasticity and reversibility of deformations.

The mechanical properties confirm the results of the TSSR analysis. Sulfur (S2) and accelerator (S3) are not sufficient to achieve a fully crosslinked material.[36] The low crosslink density can explain the compression set values as well as the elongation at break. The increase in tensile strength due to accelerators (S2a, S3, S3a) indicates a homogeneous network with active crosslinking sites and no circular bonds.[36,54]

The compound formulation with only activators and sulfur (S4) fulfills the requirements of DIN EN 681-1:200. The decrease in tensile strength when DBD was added (S4a) indicates a not fully developed network. The compression set increases as a result of the reduced crosslink density and an increase in plasticity.

Sample S5a shows a higher elongation at break than S5, but the tensile strength remains almost unchanged. The compression set values also reflect the increase in plasticity due to reducing the crosslink density indicated by TSSR.

In summary, a homogeneous rubber network with a high crosslink density is only guaranteed if all curative system components are present and act together. Although DBD can promote crosslinking of rubber, it cannot lead to a stable rubber network. DBD acts more as a crosslinking inhibitor and not as an accelerator.

3.1.3 | Effect on network formation

Due to the high number of components in rubber formulations, the mechanisms involved in vulcanization are very complex. Figure 5 shows a simplified model of the vulcanization reaction.[36] Based on the results and theoretical considerations, the potential points where DBD can interfere in the vulcanization reaction are discussed.

TABLE 5 Mechanical properties of samples S2–S5 (without DBD) and S2a–S5a (with 2.0 wt% DBD)

Samples	Compression set at 70°C for 24 h (%)	Tensile strength (MPa)	Elongation at break (%)
Reference[a]	<20	>9	>300
S2 (BC/S)	58.4	3.1	482
S2a (BC/S/DBD)	40.0	7.4	674
S3 (BC/Acc/S)	47.1	9.4	716
S3a (BC/Acc/S/DBD)	49.7	6.9	769
S4 (BC/ZS/S)	20.1	13.0	452
S4a (BC/ZS/S/DBD)	37.1	8.7	692
S5 (BC/ZS/Acc/S)	9.9	10.7	330
S5a (BC/ZS/Acc/S/DBD)	30.3	11.1	668

[a]Values of DIN EN 681-1: 2006 for O-ring sealing systems on EPDM rubber basis.

The results showed two main effects of DBD during vulcanization. The inhibition of network formation, observed by low crosslink density and stabilizing the PS crosslinks. No reversion is observed in the rheometer despite the zinc ions and PS crosslinks in S5a (TSSR). This suggests that DBD interacts with activators, as they are the reason for desulfurization and reversion.[36] Two options described in the literature might be the reason for this observation. First, PS crosslinks can be stabilized by forming Zn-DBD complexes,[17] and secondly, it is suggested that ZnO can absorb or interact with sulfur-based curative system components.[56] In either case, zinc ions can no longer promote reversion (step 3). A new crosslink precursor may not occur if zinc ions are blocked due to absorption or complexation (step 2 C). As activators lead to shorter sulfur bridges by forming new crosslink precursor, without activators, the sulfur accelerated vulcanization can be applied, leading to PS crosslinks.[36,54]

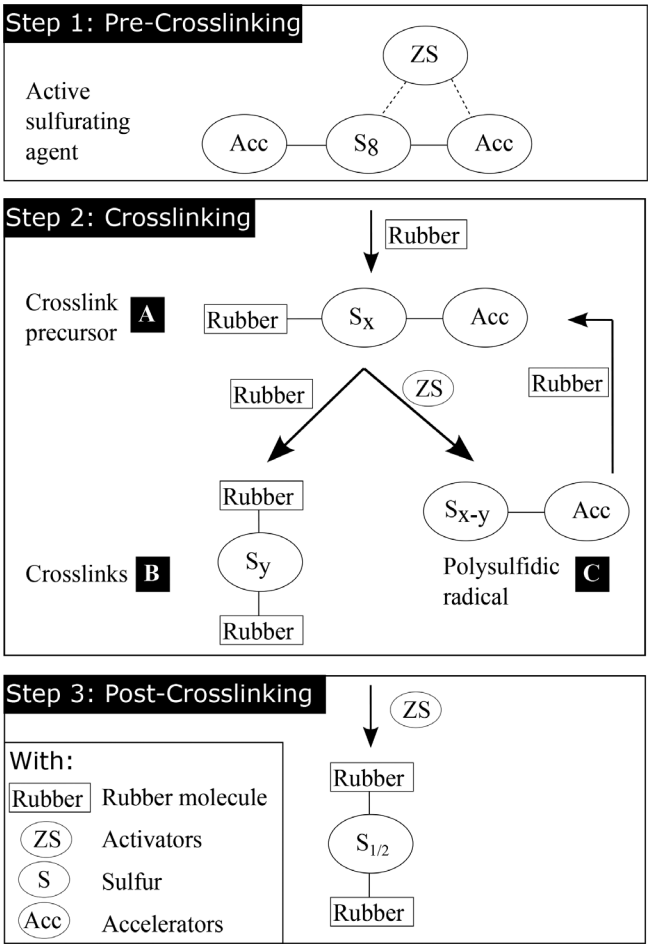

FIGURE 5 Simplified mechanism of sulfur based vulcanization reaction

Foxley investigated the accelerating function of DBD during the polymerization of styrene.[57] However, in the presence of DBD, the reaction rate was moderate, resulting in lower polymer conversion. DBD was found not to form free radicals but to act as a radical acceptor. Therefore, DBD may interact with crosslinking intermediates (step 1 and step 2 A) by the formation of complexes or by scavenging intermediate radicals, acting like a retarder or pre-vulcanization inhibitor.[36,58,59] This explains the slowed crosslinking reaction and increased scorch delay in the presence of accelerators (S3a) and activators (S4a) when DBD was added.

Since no effects on cure rate were observed when the entire curative system was used, DBD does not interfere with the crosslinking reaction. Instead, DBD radicals possibly interact with PS radicals (step 2 C), preventing MS crosslinks and resulting in low crosslink densities.

3.2 | Influence of DBD on network degradation

In Figure 6a are depicted the rheometer curves obtained at a temperature of 180°C from dry blends of RWP and different amounts of DBD.

We expected that the DBD would prevent crosslinking during network formation. In the case of S6, the rheometer torque increases because a thermal sintering process[26] takes place, and the sample is vulcanized with residues of crosslinking system in the RWP.[17,60,61] With the addition of DBD the behavior becomes different. A small amount of

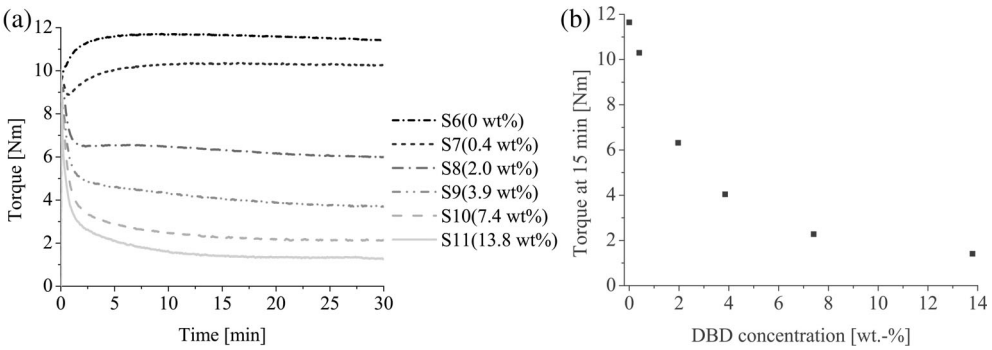

FIGURE 6 Influence of DBD concentration (a) on trace of rheometer torque of samples S6–S11 at 180°C and (b) on torque value at 15 min

DBD (S7) results in a slight decrease of torque in the initial part followed by an increase of torque, but significantly lower than without DBD. Higher concentrations of DBD (S8–S11) lead to a stronger decay of torque, indicating the degradation of the network of the RWP. The torque measured at 15 min was plotted against DBD concentrations, showing that small concentrations cause a significant decrease in torque, and higher concentrations make only a small difference (see Figure 6b). This behavior is inverse to cure behavior, where the rheometer curves exhibit an increase of torque, indicating a three-dimensional network structure formation. In another study, rheometer tests were also performed to demonstrate the devulcanization effect due to the addition of liquid metal.[62] Therefore, it can be presumed that the addition of DBD (without sulfur) leads to a degradation of a sulfur-cured EPDM network.

The influence of temperature on the degradation of the polymer network can be seen in Figure 7. The RWP blended with 3.9 wt% DBD (S9) were investigated in the temperature range from 150 to 200°C. Vulcanization and devulcanization are equilibrium processes and depend on temperature. The torque of the rheometer curve decreases with increasing temperature. Higher temperatures promote devulcanization initially. At 200°C, however, the rheometer curve rises again after about 10 min. Possibly, after reaching the maximum concentration of reactive species, recombination of radicals takes place, and vulcanization is favored.

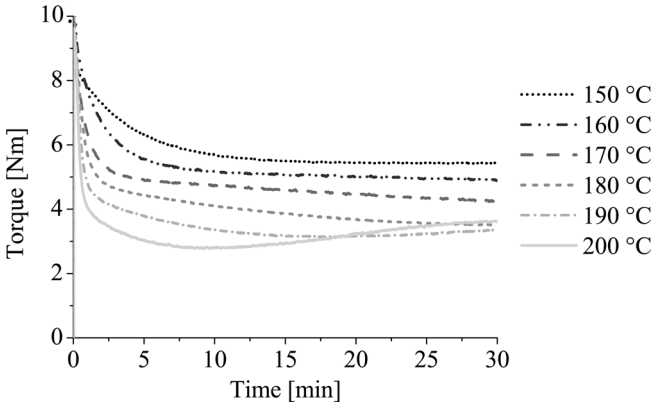

FIGURE 7 Rheometer curves at different temperatures obtained from sample S9

TABLE 6 Results of TSSR tests obtained from samples S6–S11 compression-molded at 180°C

Samples	σ_0 (MPa)	T_{50} (°C)	υ^a (mol/m^3)
S6 (0 wt%)	0.35	222.4	201
S7 (0.4 wt%)	0.30	211.8	172
S8 (2.0 wt%)	0.19	169.8	109
S9 (3.9 wt%)	0.14	133.5	80
S10 (7.4 wt%)	0.10	93.0	57
S11 (13.8 wt%)	0.09	77.8	52

[a]Calculated according to Equation (1).

3.2.1 | Effect on network structure and crosslink density

The crosslink density and the network structure of the samples S6–S11 were investigated employing TSSR measurements according to ASTM D8363-20. The values of initial stress σ_0, T_{50}, and crosslink density υ are given in Table 6.

Normalized stress temperature curves of compression-molded samples containing different concentrations of DBD are shown in Figure 8a. The RWP sample (S6) without DBD exhibits behavior like the vulcanized rubber sample (reference S5). The entropy effect is recognizable in the range from 23°C to about 40°C, and the small step about 50°C caused by polymer-filler interactions[52,53] is only observable for S6 and S7. The entropy effect is reduced or wholly suppressed in the samples containing higher DBD concentrations (S8–S11).

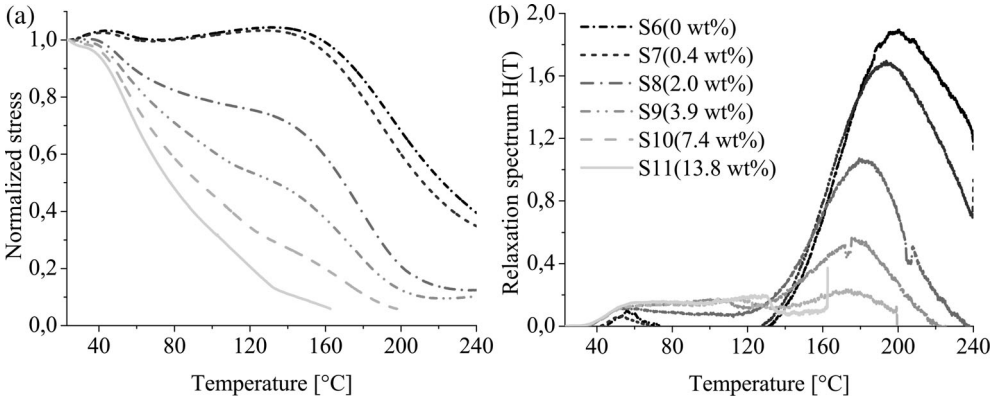

FIGURE 8 TSSR stress temperature curves (a) and relaxation spectra (b) of samples S6–S11

High DBD concentrations lead to strong stress relaxation, which is comparable to the typical behavior of thermoplastic rubber with high plasticity.[55]

Figure 8b shows the corresponding relaxation spectra of compression-molded samples containing different concentrations of DBD. The RWP was obtained by grinding an EPDM rubber compound initially cured by an EV sulfur cure system. Therefore, it is presumed that the RWP network consists mainly of MS and DS bridges. RWP without DBD (S6) shows a broad relaxation peak containing bridges with different amounts of sulfur atoms. Short sulfur bridges like MS and DS crosslinks are indicated by the peak position at a high temperature and a high T_{50} value (Table 6). The addition of DBD leads to a decrease of the relaxation peak height at high temperatures and a shift of the peak position, which is related to the cleavage of MS and DS crosslinks. The decrease of thermal stability and crosslinks by an increase of DBD concentration is also observed by decreasing the T_{50} values (Figure 9).

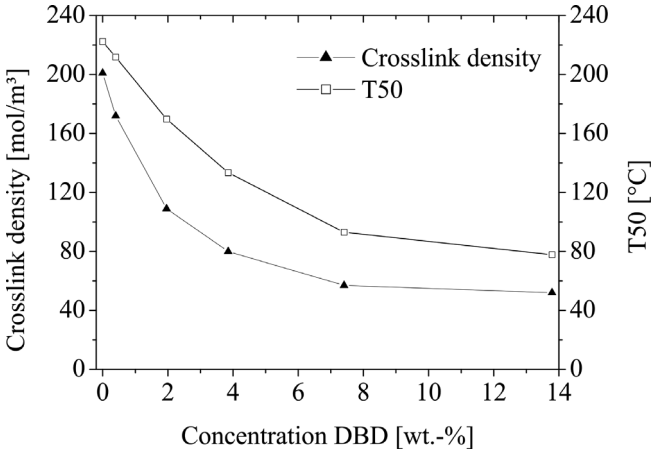

FIGURE 9 Influence of DBD concentration (S6–S11) on crosslink density and T_{50}-value

In conclusion, the MS bridges are degraded more efficiently by a low concentration of DBD. To degrade the PS bridges, higher amounts of DBD are necessary. The network degradation by adding DBD is also indicated by the decrease of crosslink density, depicted in Figure 9.

The T_{50} value and the crosslink density are a function of DBD concentration. These observations agree with a previous study where an EV cured EPDM with mainly MS and DS crosslinks was better devulcanized with DPDS and DBD than a conventionally (CONV) cured EPDM with mainly PS crosslinks.[18] The lower crosslink density of the EV cured rubber compared to the CONV cured EPDM was advantageous to the better degradation result.

The stress curves and relaxation spectra of S9 compression-molded at different temperatures are shown in Figure 10. The values of initial stress, T_{50}, and crosslink density are given in Table 7.

The normalized stress curve shows no difference between the samples treated at different temperatures during thermo-chemical devulcanization (see Figure 10a). On the other hand, the relaxation peaks in the relaxation spectra (see Figure 10b) present a shift to the right. This means that the crosslinks are more thermally stable the higher the devulcanization temperature was. However, higher temperatures lead to more network degradation, as evidenced by the decrease in crosslink density (Table 7). Nevertheless, the influence of devulcanization temperature on crosslink density (Table 7) is small compared to the effect of DBD concentration (Table 6).

3.2.2 | Effect on mechanical properties

Mechanical properties were determined on samples S6–S11 compression-molded at 180°C (see Table 8). The compression set increases with an increase in DBD concentration. It is expected that the plasticity is

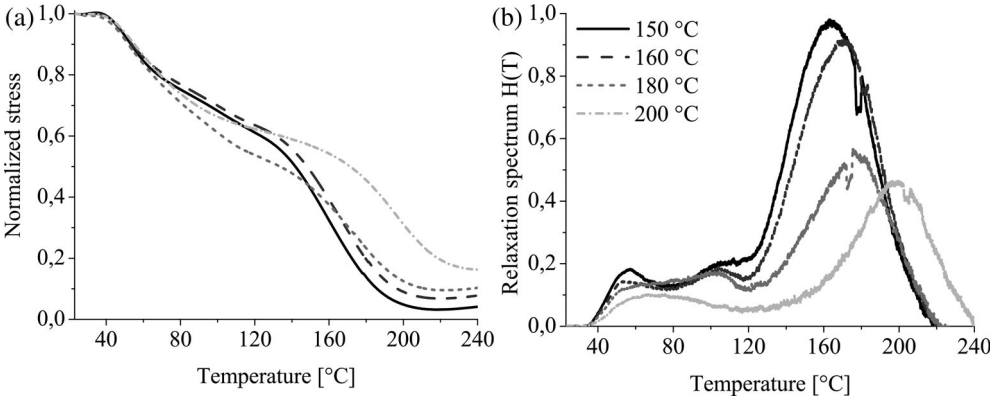

FIGURE 10 TSSR stress temperature curves (a) and relaxation spectra (b) of sample S9 compression-molded at different temperatures

increasing, and the elasticity is decreasing due to network degradation.

The stress–strain curves are depicted in Figure 11. Higher DBD concentrations lead to higher network degradation, resulting in higher tensile strength and elongation at break. If the network is degraded too much, the tensile strength and elongation at break decreased.

3.2.3 | Effect on network degradation

The TSSR measurements and rheometer curves show that DBD in combination with temperature leads to network degradation without mechanical shearing force.

Since the samples were compression molded, rearrangement of the crosslinks may occur as described for the high-pressure high-temperature sintering (HPHTS) process.[26] In literature, the function of disulfides is mainly considered as radical scavengers.[38] Therefore, DBD radicals can scavenge radicals generated during the rearrangement of crosslink bridges. Since DBD first specifically degrades MS crosslinks, it is conceivable that DBD acts as a radical scavenger and a cleavage reagent. From a chemical point of view, the radical scission mechanism proposed by Joseph et al. for NR[32] can also be applied to EPDM. The thermomechanically induced disulfide radical cleaves the sulfur crosslinks by attacking double bonds adjacent to crosslinks. The thiophenol radical abstracts one H atom from the polymer chain. The sulfide radical splits off, creating a new active crosslinking site that can be re-crosslinked. Radical scavenging as well as cleavage are both feasible and can co-occur during thermo-chemical devulcanization. Both pathways have in common that they lead to a reduced crosslink density. Although residues of the curative system[17,60,61] and double bonds[63] are present in the RWP, DBD can react with the crosslinking intermediates as observed during vulcanization, leading to fewer crosslinks.

The network degradation is dependent on the concentration of DBD and temperature. The MS bridges are favorably degraded at lower concentrations, while the PS bridges are degraded at higher DBD concentrations. The literature describes the opposite: PS bridges are more easily cleaved compared to MS bridges due to the difference in binding energies.[36,37] Also, the described model of delocalization of electron radicals during the mechanical cleavage of sulfidic crosslinks would favor the degradation of PS crosslinks since the formed radicals are better delocalized during the cleavage of PS crosslinks.[64] However, Dijkhuis found that CONV cured EPDM was more difficult to degrade than EV cured EPDM.[18] Gehrke et al. pointed out that the angular conformations of S-S are close to ideal at the tetrahedral angle.[64] Therefore, it is possible that the energy of the PS bridges may be lower, and DBD prefers to attack the MS crosslinks.

TABLE 7 Results of TSSR tests obtained from sample S9 compression-molded at 150, 160, 180, and 200°C

Samples	σ_0 (MPa)	T_{50} (°C)	υ^a (mol/m^3)
S9 (150°C)	0.20	141.9	115
S9 (160°C)	0.18	148.2	103
S9 (180°C)	0.14	133.5	80
S9 (200°C)	0.10	171.3	57

[a]Calculated according to Equation (1).

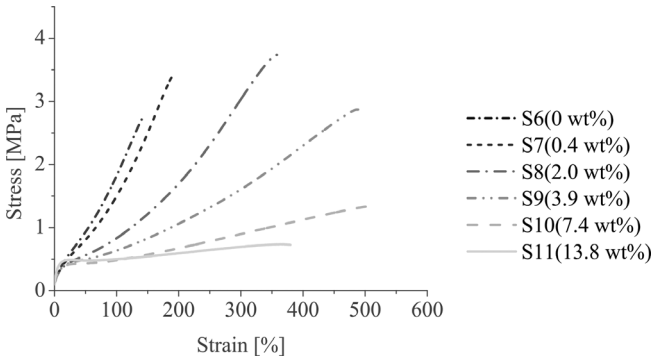

FIGURE 11 Influence of DBD concentration on stress–strain curves of samples S6–S11

TABLE 8 Mechanical properties of samples S6–S11 cured at 180°C

Samples	Compression set at 70°C for 24 h (%)	Tensile strength (MPa)	Elongation at break (%)
Reference S5	9.9	10.7	330
S6 (0 wt%)	14.4	2.8	144
S7 (0.4 wt%)	16.7	3.4	193
S8 (2.0 wt%)	31.4	3.7	358
S9 (3.9 wt%)	59.9	2.9	491
S10 (7.4 wt%)	76.5	1.4	519
S11 (13.8 wt%)	91.5	0.7	380

Furthermore, the PS bridges can be stabilized by complexation[17] leaving the MS crosslinks to be attacked.

The mechanical tests show an improvement in properties by increasing the DBD concentration despite the degradation of the network. Two types must be distinguished concerning the network: the intraparticle network (in the particles) and the interparticle network (between the particles). When the RWP are pressed together in the heating press, the particles react at the interface, forming a composite (interparticle network). Degradation of the network can create free chain ends at the edge of the particles that form bonds with neighboring particles, strengthening the composite (interparticle network). This is one possible explanation for better mechanical properties. Another reason may be the different crosslinking densities of the two network types. It has been reported that other crosslinked regions in a rubber network, referred to as network inhomogeneities, affect mechanical properties.[51,65] Thus, non-dispersed crosslinked domains in the network can be considered weak points that negatively influence the stress transfer and thus decrease tensile strength.[66] Conversely, it can be concluded that by reducing the crosslink density in the particles, that is, degradation of the intraparticle network, the entire network becomes more homogeneous and uniform, leading to better tensile properties. In addition, with fewer crosslinking sites, the polymer chains have higher mobility, resulting in higher elongation at break.[41,45]

4 | CONCLUSION

In this study, the influence of DBD on network formation (vulcanization) and network degradation (devulcanization) was investigated. DBD acts as an accelerator during vulcanization if the cure system contains only sulfur but no other additives or activators, for example, ZnO or stearic acid. DBD acts as a retarder or pre-vulcanization inhibitor when the accelerator is added, which is observed by an increase in scorch time and a decrease in cure rate. In the presence of activators, DBD leads to a distinct reduction in crosslink density. Scorch time and cure rates are also affected. The EV curative system leads to low crosslink density and predominantly PS bonds formation in the presence of DBD. Strong interaction of DBD and the curative system take place. DBD can be complexed or absorbed by zinc and react with radical vulcanization intermediates, preventing the formation of MS crosslinks. The consequence is an elastomeric composite with low crosslinking density, high elongation at break, and poor compression set values. But the efficiency of the devulcanization depends strongly on the temperature and DBD concentration. The TSSR measurements give an insight into the network structure during devulcanization. The rheometer curves and TSSR measurements show an evident degradation of the rubber network, that is, devulcanization even at temperatures below 200°C. The relaxation spectra show DBD first cleaves the MS crosslinks, and the PS crosslinks are cleaved at higher concentrations. Since cleavage is quite specific, it is feasible that DBD acts not only as a radical scavenger but also as a cleavage reagent. The decrease in crosslink density due to cleavage of sulfur bonds by DBD leads to plastification of the rubber waste, which is reflected in the compression set values and elongation at break. The tensile strength is improved as network inhomogeneities caused by areas with different crosslink densities are reduced due to degradation. The results show that DBD is an effective devulcanizing agent at temperatures below 200°C. The mild reaction conditions protect the polymer backbone, save energy during processing, and make rubber recycling attractive and suitable for new industrial rubber goods and composites.

ACKNOWLEDGMENTS

This work was financially supported by the German Federal Environmental Foundation grant number 34250/01-21/0. We would like to thank Prof. Markus Susoff for the opportunity to work in the Laboratory for Rubber Technology of the Faculty of Engineering and Computer Science at the University of Applied Sciences Osnabrueck. The authors are also grateful to the companies M.D.S. Meyer and Schill & Seilacher for providing the materials needed for this project.

AUTHOR CONTRIBUTIONS

Larissa Gschwind: Writing – original draft (lead). **Simona Jordan:** Writing – review and editing (supporting). **Norbert Vennemann:** Writing – review and editing (supporting).

DATA AVAILABILITY STATEMENT

Research data are not shared.

ORCID

Larissa Gschwind https://orcid.org/0000-0001-5767-977X

Carmen-Simona Jordan https://orcid.org/0000-0002-4354-4484

Norbert Vennemann https://orcid.org/0000-0001-8913-7895

REFERENCES

[1] E. Bilgili, H. Arastoopour, B. Bernstein, *Powder Technol.* **2001**, *115*, 277.

[2] H. Yazdani, M. Karrabi, I. Ghasmi, H. Azizi, G. R. Bakhshandeh, *J. Vinyl Addit. Technol.* **2011**, *17*, 64.

[3] N. Kawabata, S. Yamashita, Y. Furukawa, *Bull. Chem. Soc. Jpn.* **1978**, *51*, 625.
[4] C. G. Moore, B. R. Trego, *J. Appl. Polym. Sci.* **1964**, *8*, 1957.
[5] S. Rooj, G. C. Basak, P. K. Maji, A. K. Bhowmick, *J. Polym. Environ.* **2011**, *19*, 382.
[6] V. Tatangelo, I. Mangili, P. Caracino, M. Anzano, Z. Najmi, G. Bestetti, E. Collina, A. Franzetti, M. Lasagni, *Appl. Microbiol. Biotechnol.* **2016**, *100*, 8931.
[7] F. Ghavipanjeh, Z. Ziaei Rad, M. Pazouki, *J. Polym. Environ.* **2018**, *26*, 3168.
[8] A. Ali Shah, F. Hasan, Z. Shah, N. Kanwal, S. Zeb, *Int. Biodeterior. Biodegrad.* **2013**, *83*, 145.
[9] J. Yun, V. V. Yashin, A. I. Isayev, *J. Appl. Polym. Sci.* **2004**, *91*, 1646.
[10] A. I. Isayev, S. P. Yushanov, S. H. Kim, V. Y. Levin, *Rheol. Acta* **1996**, *35*, 616.
[11] V. Pistor, C. H. Scuracchio, P. J. Oliveira, R. Fiorio, A. J. Zattera, *Polym. Eng. Sci.* **2011**, *51*, 697.
[12] F. D. B. de Sousa, J. R. Gouveia, P. M. F. de Camargo Filho, S. E. Vidotti, C. H. Scuracchio, L. G. Amurin, T. S. Valera, *Polimeros* **2015**, *25*, 256.
[13] X. Colom, J. Canavate, K. Formela, A. Shadman, M. R. Saeb, *Polym. Degrad. Stab.* **2021**, *183*, 109450.
[14] V. Lapkovskis, V. Mironovs, A. Kasperovich, V. Myadelets, D. Goljandin, *Recycling* **2020**, *5*, 32.
[15] J. W. M. Noordermeer, W. Dierkes, A. Blume, K. Dijkhuis, H. van Hoek, L. Reuvekamp, S. Saiwari, *Rubber World* **2020**, *262*, 20.
[16] X. L. Lv, H. X. Huang, B. Y. Lv, *J. Appl. Polym. Sci.* **2016**, *133*, 761.
[17] V. Rajan, Ph.D. Thesis, University of Twente, **2005**.
[18] K. A. J. Dijkhuis, Ph.D. Thesis, University of Twente, **2008**.
[19] S. G. Butuc, A. Janssen, K. van Leerdam, A. Talma, A. Blume, *Rubber Plast. News* **2020**, February 10. https://s3-prod.rubbernews.com.
[20] P. Sutanto, F. L. Laksmana, F. Picchioni, L. P. B. M. Janssen, *Chem. Eng. Sci.* **2006**, *61*, 6442.
[21] A. Macsiniuc, A. Rochette, D. Rodrigue, *Prog. Rubber Plast. Recycl. Technol.* **2010**, *26*, 51.
[22] M. Mouri, N. Sato, H. Okamoto, M. Matsushita, H. Honda, K. Nakashima, K. Takeushi, Y. Suzuki, M. Owaki, *Int. Polym. Sci. Technol.* **2000**, *27*, T17.
[23] S. Teich, E. Haberstroh, U. Giese, *J. Appl. Polym. Sci.* **2022**, *139*, 520.
[24] K. Fukumori, M. Matsushita, M. Mouri, H. Okamoto, N. Sato, K. Takeuchi, Y. Suzuki, *Kautschuk Gummi Kunststoffe* **2006**, *59*, 405.
[25] E. Finazzi, A. Gallo, P. Lucci, *Rubber World* **2011**, *244*, 21.
[26] J. E. Morin, D. E. Williams, R. J. Farris, *Rubber Chem. Technol.* **2002**, *75*, 955.
[27] A. R. Tripathy, J. E. Morin, D. E. Williams, S. J. Eyles, R. J. Farris, *Macromolecules* **2002**, *35*, 4616.
[28] O. Buitrago-Suescún, R. Britto, *Iran. Polym. J.* **2020**, *29*, 553.
[29] S. Seghar, N. A. Hocine, V. Mittal, S. Azem, F. Al-Zohbi, B. Schmaltz, N. Poirot, *Express Polym. Lett.* **2015**, *9*, 1076.
[30] S. Ostad Movahed, A. Ansarifar, S. Estagy, *Rubber Chem. Technol.* **2016**, *89*, 54.
[31] M. A. L. Verbruggen, L. van der Does, J. W. M. Noordermeer, M. van Duin, *J. Appl. Polym. Sci.* **2008**, *109*, 976.
[32] A. M. Joseph, B. George, K. Madhusoodanan, R. Alex, *Rubber Sci.* **2016**, *29*, 62.
[33] D. M. Beaupre, R. G. Weiss, *Molecules* **2021**, *26*, 3332.
[34] M. Myhre, S. Saiwari, W. Dierkes, J. Noordermeer, *Rubber Chem. Technol.* **2012**, *85*, 408.
[35] M. van Duin, J. W. M. Noordermeer, M. A. L. Verbruggen, L. van der Does, DSM IP Assets B.v., Heerlen, US6956065B2, **2005**.
[36] A. M. Joseph, B. George, K. N. Madhusoodanan, R. Alex, *Rubber Sci.* **2015**, *28*, 82.
[37] W. K. Dierkes, V. V. Rajan, J. Noordermeer, *Kautschuk Gummi Kunststoffe* **2005**, *58*, 312.
[38] S. Ostad Movahed, A. Ansarifar, S. Karbalaee, S. Athary Far, *Prog. Rubber Plast. Recycl. Technol.* **2015**, *31*, 87.
[39] D. De, S. Maiti, B. Adhikari, *J. Appl. Polym. Sci.* **1999**, *73*, 2951.
[40] S. K. Mandal, N. Alam, S. C. Debnath, *Rubber Chem. Technol.* **2012**, *85*, 629.
[41] J. Ghosh, S. Ghorai, S. Bhunia, M. Roy, D. De, *Polym. Eng. Sci.* **2018**, *58*, 74.
[42] B. C. Sekhar, V. A. Kormer, E. N. Sotnikova, V. P. Mironyuk, L. N. Trunova, N. A. Nikitina, US5770632, **1998**.
[43] A. R. Jalilvand, I. Ghasemi, M. Karrabi, H. Azizi, *Iran. Polym. J.* **2007**, *16*, 327.
[44] S. Ostad Movahed, A. Ansarifar, G. Zohuri, N. Ghaneie, Y. Kermany, *J. Elastomers Plast.* **2016**, *48*, 122.
[45] S. Saiwari, K. Waesateh, A. Worlee, N. Hayeemasae, C. Nakason, *Kautschuk Gummi Kunststoffe* **2019**, *72*, 35.
[46] S. Hoyer, L. Kroll, D. Sykutera, *Proc. Manuf.* **2020**, *43*, 193.
[47] A. M. Lepadatu, S. Asaftei, N. Vennemann, *J. Appl. Polym. Sci.* **2015**, *132*, 32.
[48] N. Vennemann, C. Schwarze, C. Kummerlöwe, *Adv. Mater. Res.* **2014**, *844*, 482.
[49] L. González, A. Rodríguez, A. Del Campo, A. Marcos-Fernández, *J. Appl. Polym. Sci.* **2002**, *85*, 491.
[50] B. Vega, L. Montero, S. Lincoln, N. Agulló, S. Borrós, *J. Appl. Polym. Sci.* **2008**, *108*, 1969.
[51] Y. Ikeda, N. Higashitani, K. Hijikata, Y. Kokubo, Y. Morita, M. Shibayama, N. Osaka, T. Suzuki, H. Endo, S. Kohjiya, *Macromolecules* **2009**, *42*, 2741.
[52] N. Vennemann, M. Wu, M. Heinz, *Kautschuk Gummi Kunst.* **2011**, *64*, 40.
[53] N. Vennemann, M. Wu, M. Heinz, *Rubber World* **2012**, *246*, 18.
[54] J. W. M. Noordermeer, Vulcanization. in *Encyclopedia of Polymeric Nanomaterials* (Eds: S. Kobayashi, K. Müllen), Springer, Berlin **2015**.
[55] A. Barbe, K. Bökamp, C. Kummerlöwe, H. Sollmann, N. Vennemann, S. Vinzelberg, *Polym. Eng. Sci.* **2005**, *45*, 1498.
[56] R. Steudel, Y. Steudel, *Chem. A Eur. J.* **2006**, *12*, 8589.
[57] G. H. Foxley, *J. Polym. Sci.* **1959**, *41*, 545.
[58] V. Ducháček, *J. Appl. Polym. Sci.* **1972**, *16*, 3245.
[59] D. G. H. Ballard, J. Myatt, J. F. P. Richter, *J. Appl. Polym. Sci.* **1972**, *16*, 2647.
[60] A. M. Lepadatu, S. Asaftei, N. Vennemann, *Kautschuk Gummi Kunststoffe* **2014**, *67*, 41.
[61] A. M. Joseph, B. George, K. N. Madhusoodanan, R. Alex, *Rubber Chem. Technol.* **2017**, *90*, 536.
[62] S. S. Banerjee, A. Das and A. Fery, Leibniz Inst. Polymerforschung Dresden DE Ger. 102020117045B3, **2021**.
[63] A. Amash, U. Giese, R. H. Schuster, *Kautschuk Gummi Kunststoffe* **2002**, *55*, 218.
[64] S. Gehrke, H. T. Alznauer, H. A. Karimi-Varzaneh, J. A. Becker, *J. Chem. Phys.* **2017**, *147*, 214703.
[65] S. Saiwari, Ph.D. Thesis, University of Twente, **2013**.
[66] G. K. Jana, C. K. Das, *Macromol. Res.* **2005**, *13*, 30.

SUPPORTING INFORMATION

Additional supporting information may be found in the online version of the article at the publisher's website.

How to cite this article: L. Gschwind, C.-S. Jordan, N. Vennemann, *J. Appl. Polym. Sci.* **2022**, e52141. https://doi.org/10.1002/app.52141